

Leptogenesis and Neutrinoless Double Beta in the Scotogenic Hybrid Textures of Neutrino Mass Matrix

Ankush*, Rishu Verma[†], Sahil Kumar[‡] and B. C. Chauhan[§]

*Department of Physics and Astronomical Science,
Central University of Himachal Pradesh, Dharamshala 176215,
INDIA.*

Abstract

In our recent work we identify the hybrid textures which simultaneously account for dark matter (DM), neutrinoless double beta decay ($0\nu\beta\beta$) and leptogenesis. We also obtained the bounds on dark matter mass and effective Majorana mass $|M_{ee}|$. We have found correlation of baryon asymmetry of universe Y with dark matter mass M_1 and effective Majorana mass $|M_{ee}|$. We use experimental bounds on relic density of dark matter (Ωh^2) and baryon asymmetry of universe to identify the hybrid textures. We found that out of five hybrid textures which simultaneously satisfies the physics observations of the DM and $0\nu\beta\beta$ only three hybrid textures altogether satisfy the DM, $0\nu\beta\beta$ and leptogenesis. It is interesting to note that these three hybrid textures gives lower bound to the effective Majorana mass $|M_{ee}|$ which can be probed in current and future experiments like SuperNEMO, KamLAND-Zen, NEXT, and nEXO (5 year) have sensitivity reaches of 0.05 eV, 0.045 eV, 0.03 eV, and 0.015 eV, respectively.

1 Introduction

We are aware of recent developments in the theory and experiments of fundamental particles and their interactions at electroweak scale. In the present scenario, it is unquestionably incomplete to solve the puzzles like non vanishing neutrino mass, existence of dark matter and baryon asymmetry of universe (BAU). Therefore, a conclusive theory to accommodate all these phenomena hints towards the physics beyond standard model (BSM). The history of neutrino oscillation experiments over the last few decades has confirmed that neutrinos are not massless but have a tiny

*ankush.bbau@gmail.com

[†]rishuvrm274@gmail.com

[‡]sahilruhaan1999@gmail.com

[§]bcawake@hpcu.ac.in

mass. However, these oscillation experiments are only sensitive to the mass square differences and inert to absolute mass scale of the neutrinos. Moreover, the upper limit to the sum of neutrino mass is $\sum M_\nu \leq 0.12$ eV [1].

The data from cosmological and astrophysical observations of gravitational lensing, galaxy rotation curves, cosmic microwave background (CMBR) and large scale structure formation etc confirm the evidences of the dark matter in the universe. With current abundance

$$\Omega h^2 = 0.120 \pm 0.001,$$

DM contributes to the 26.8% of the total energy density of the present universe as evident from PLANCK [1]. As we know, we don't have any formalism in SM to include DM so that it would be stable on the cosmological time scale. However, there exist some BSM frameworks which could stabilize the DM by the inclusion of additional symmetries to the radiative or tree-level models [2,3]. One of such models is at one loop level which we are going to implement in our study is scotogenic model that simultaneously explains the DM and small neutrino mass [4].

There is ambiguity that whether neutrinos are four component Dirac particles or two component Majorana particles. This ambiguity will become clear once experiments confirm or reject neutrinoless double beta ($0\nu\beta\beta$) decay. This decay would also confirm that the neutrino is its own antiparticle. Furthermore, it would be evidence of lepton number violation and could aid in determining the absolute neutrino mass scale. In fact, there is currently no experimental evidence for this decay. However, with the advancement of future experimental techniques, we hope to see some interesting results.

The Big Bang theory proposes symmetric initial conditions for particles and antiparticles. Therefore, as a result of the annihilation effects, no matter would remain. However, what we observe in today's universe is matter dominance, which is referred to as baryon asymmetry of the universe. Non-symmetric initial conditions, on the other hand, are ineffective in the Standard Model of elementary particle physics due to the inflationary phase and nonperturbative effects. Hence, it is clear that this asymmetry is dynamically generated. However, we don't know where it originated from. The current cosmological bound for baryon asymmetry is [1]

$$Y = (6.04 \pm 0.08) \times 10^{-10}.$$

The small neutrino mass can be generated primarily in two ways, 1) by using a traditional tree-level seesaw models [5–9], and 2) by using a radiative mechanism. The radiative models are more promising because the new particles introduced in these models are very much lighter in comparison to particles involved in the conventional seesaw mechanism. Radiative neutrino mass generation is possible at one-loop [10–15], two-loop [16–20], three-loop [21–26], and higher-loop levels. The interesting feature of radiative model is the suppression in the mass of the neutrino at n-loop level varies as (suppression)ⁿ [27]. As a result, with larger loops, these particles can be easily tested at the LHC. In our investigation, we employ the well-known radiative model called scotogenic model for neutrino mass generation [4]. The merit of using this model is that it simultaneously account for the neutrino mass and dark matter. The implications of the model to the texture zeros are discussed in Refs [28–30].

In this work, we make an effort to explain the dark matter, neutrinoless double beta decay and leptogenesis in a single framework under the assumption that the neutrino is a Majorana particle. We operate within a more restrictive framework in the one loop level and hybrid textures in the neutrino mass matrix. Hybrid textures are the ones with one ‘zero’ and one ‘equality’ in the neutrino mass matrix [31–35]. Here, all elements of neutrino mass matrix are expressed as proportional to the non-zero $|M_{ee}|$ element of the neutrino mass matrix as discussed in our previous work [30]. This is one of the key characteristics of hybrid textures taken into consideration in this work.

The paper is organized as follows: In Section 2, we outline the Scotogenic model and relic density of the dark matter, The Section 3 discusses the dark matter and $0\nu\beta\beta$ decay in the hybrid textures of neutrino mass matrix and the lepton asymmetry is discussed in section 4. Section 5 discusses the specifics of the numerical analysis and interpretations of the phenomenological results. Finally, in Section 6, the conclusions are explained.

2 Scotogenic model and relic density of the dark matter

In this model, we add three right-handed singlet fermions $N_k (k = 1, 2, 3)$ which are singlet under $SU(2)_L$ and an $SU(2)_L$ scalar doublet (η^+, η^0) to the standard model (SM) which are odd under exact Z_2 symmetry [4]. The particle content of the model under $SU(2)_L \times U(1)_Y \times Z_2$ is given by

$$\begin{aligned} L_\alpha &= (\nu_\alpha, l_\alpha) : (2, -1/2, +), l_\alpha^C : (1, 1, +), \\ \phi &= (\phi^+, \phi^0) : (2, -1/2, +), \\ \eta &= (\eta^+, \eta^0) : (2, 1/2, -), N_k : (1, 0, -), \end{aligned} \quad (1)$$

where $\alpha = e, \mu, \tau$, (ν_α, l_α) and (ϕ^+, ϕ^0) are left-handed lepton doublets and Higgs doublet, respectively.

The Lagrangian of the model with relevant Yukawa and mass terms is given by

$$\mathcal{L} \supset Y_{\alpha k} (\bar{\nu}_{\alpha L} \eta^0 - \bar{l}_{\alpha L} \eta^+) N_k + \frac{1}{2} M_k \bar{N}_k N_k^C + H.c., \quad (2)$$

and the relevant scalar potential interaction terms are given by

$$V \supset \frac{1}{2} \lambda (\phi^\dagger \eta)^2 + h.c., \quad (3)$$

where λ is the quartic coupling. The presence of exact Z_2 symmetry forbids the neutrinos to acquire mass at tree level and neutrino mass is thus generated radiatively at one loop level. The general element of neutrino mass matrix $M_{\alpha\beta}$ is given by

$$M_{\alpha\beta} = \sum_{k=1}^3 Y_{\alpha k} Y_{\beta k} \Lambda_k, \quad (4)$$

where

$$\Lambda_k = \frac{\lambda v^2}{16\pi^2} \frac{M_k}{m_0^2 - M_k^2} \left(1 - \frac{M_k^2}{m_0^2 - M_k^0} \ln \frac{m_0^2}{M_k^2} \right), \quad (5)$$

$$m_0^2 = \frac{1}{2}(m_R^2 + m_I^2), \quad (6)$$

where $v = 246\text{GeV}$, is the vacuum expectation value (vev) of the Higgs field, m_R , m_I and $M_k (k = 1, 2, 3)$ are the masses of $\sqrt{2}Re[\eta^0]$, $\sqrt{2}Im[\eta^0]$ and right-handed neutrino respectively. The lepton flavor violating (LFV) processes such as $\mu \rightarrow e\gamma$ is induced at one loop level. Thus the branching ratio for $\mu \rightarrow e\gamma$ process is given as [12, 13]

$$Br(\mu \rightarrow e\gamma) = \frac{3\alpha_{em}}{64\pi(G_F m_0^2)^2} \left| \sum_{k=1}^3 Y_{\mu k} Y_{ek}^* F\left(\frac{M_k}{m_0}\right) \right|^2, \quad (7)$$

where α_{em} is the fine structure constant for electromagnetic coupling, G_F is Fermi coupling constant and $F(r)$ is given as

$$F(r) = \frac{1 - 6r^2 + 3r^4 + 2r^6 - 6r^4 \ln r^2}{6(1 - r^2)^4}, \quad r \equiv \frac{M_k}{m_0}. \quad (8)$$

It is interesting to note that this model provides the simultaneous measurement of DM and neutrino mass. Being Z_2 odd, the lightest of N_k will be the stable DM candidate. Taking into account the coannihilation effect [36], the predicted cold dark matter abundance as well as the branching ratio of the lepton-flavor-violating (LFV) $\mu \rightarrow e\gamma$ process can be consistent with observations, within model at the same time. Here we consider mass of the lightest N_k (DM) is nearly degenerate with the next singlet fermion N_2 and the right-handed neutrino mass spectrum considered is $M_1 \leq M_2 < M_3$ [37]. The product of co-annihilation cross-section and relative velocity of annihilating particle v_r is given by [38]

$$\sigma_{ij}|v_r| = a_{ij} + b_{ij}v_r^2, \quad (9)$$

where

$$\left. \begin{aligned} a_{ij} &= \frac{1}{8\pi} \frac{M_1^2}{(M_1^2 + m_0^2)^2} \sum_{\alpha, \beta} (Y_{\alpha i} Y_{\beta j} - Y_{\alpha j} Y_{\beta i})^2, \\ b_{ij} &= \frac{m_0^4 - 3m_0^2 M_1^2 - M_1^4}{3(M_1^2 + m_0^2)^2} a_{ij} + \frac{1}{12\pi} \frac{M_1^2 (M_1^4 + m_0^4)}{(M_1^2 + m_0^2)^4} \sum_{\alpha, \beta} Y_{\alpha i} Y_{\alpha j} Y_{\beta i} Y_{\beta j}, \end{aligned} \right\}. \quad (10)$$

Here $\sigma_{ij} (i, j = 1, 2)$ in Eqn. (9) represents the annihilation cross-section for the process $N_i N_j \rightarrow xx'$, $dM = (M_2 - M_1)/M_1$ is the mass splitting ratio for the nearly degenerate singlet fermions, $x = M_1/T$ i.e. ratio of DM mass to the temperature T . If g_1, g_2 represent the number of degrees of freedom of singlet fermions N_1 and N_2 , respectively, the effective cross section is given by

$$\sigma_{eff} = \frac{g_1^2}{g_{eff}^2} \sigma_{11} + \frac{2g_1 g_2}{g_{eff}^2} \sigma_{12} (1 + dM)^{3/2} \exp(-xdM) + \frac{g_2^2}{g_{eff}^2} \sigma_{22} (1 + dM)^3 \exp(-2xdM), \quad (11)$$

$$g_{eff} = g_1 + g_2 (1 + dM)^{3/2} \exp(-xdM), \quad (12)$$

with $dM \simeq 0$ (N_1 is nearly degenerate with N_2) and using Eqns.(9) and (12) in Eqn.(11) we get

$$\sigma_{eff}|v_r| = \left(\frac{\sigma_{11}}{4} + \frac{\sigma_{12}}{2} + \frac{\sigma_{22}}{4} \right) |v_r|, \quad (13)$$

$$= a_{eff} + b_{eff}v_r^2,$$

where

$$\left. \begin{aligned} a_{eff} &= \frac{a_{11}}{4} + \frac{a_{12}}{2} + \frac{a_{22}}{4}, \\ b_{eff} &= \frac{b_{11}}{4} + \frac{b_{12}}{2} + \frac{b_{22}}{4}, \end{aligned} \right\}. \quad (14)$$

The thermal average cross section is

$$\langle \sigma_{eff}|v_r| \rangle = a_{eff} + 6b_{eff}/x, \quad (15)$$

which has dependence on temperature through the relation $x = M_1/T$ and relic density of cold dark matter is given by

$$\Omega h^2 = \frac{1.07 \times 10^9 \text{GeV}^{-1} x_f}{(a_{eff} + 3b_{eff}/x_f) g_*^{1/2} m_{Pl}}, \quad (16)$$

where $m_{Pl} = 1.22 \times 10^{19} \text{GeV}$, $g_* = 106.75$ and

$$x_f = \ln \frac{0.038 g_{eff} m_{Pl} M_1 \langle \sigma_{eff}|v_r| \rangle}{g_*^{1/2} x_f^{1/2}}. \quad (17)$$

Also $x_f = M_1/T_f \approx 25$, T_f is the freeze-out temperature [39].

3 Dark matter and $0\nu\beta\beta$ decay in the hybrid textures of neutrino mass matrix

The general neutrino mass matrix is written as

$$M_\nu = U \text{diag}(m_1, m_2 e^{i\alpha_2}, m_3 e^{i\alpha_3}) U^T \equiv \begin{pmatrix} M_{ee} & M_{e\mu} & M_{e\tau} \\ M_{e\mu} & M_{\mu\mu} & M_{\mu\tau} \\ M_{e\tau} & M_{\mu\tau} & M_{\tau\tau} \end{pmatrix}, \quad (18)$$

where U is the Pontecorvo–Maki–Nakagawa–Sakata (PMNS) mixing matrix, (m_1, m_2, m_3) are three neutrino mass eigenvalues and (α_2, α_3) are Majorana phases. In general, the matrix U is parameterized in term of three mixing angles $(\theta_{12}, \theta_{23}, \theta_{13})$ and one Dirac CP violating phase δ . Therefore, the elements of the the neutrino mass matrix are functions of total nine parameters viz. three mass eigen values (m_1, m_2, m_3) , three mixing angles $(\theta_{12}, \theta_{23}, \theta_{13})$, two majorana phases (α_2, α_3) and one Dirac CP phase δ as shown below

$$M_{\alpha\beta} = f(m_1, m_2, m_3, \theta_{12}, \theta_{23}, \theta_{13}, \alpha_2, \alpha_3, \delta). \quad (19)$$

Also the μ - τ sector is expressed as function of M_{ee} , $M_{e\mu}$, $M_{e\tau}$ three mixing angles $(\theta_{12}, \theta_{23}, \theta_{13})$ and one Dirac CP phase δ as [40, 41]

$$M_{\mu\tau} = f(M_{ee}, M_{e\mu}, M_{e\tau}, \theta_{12}, \theta_{23}, \theta_{13}, \delta). \quad (20)$$

For example

$$\begin{aligned}
M_{\mu\mu} &= (a + b \cos 2\theta_{23})M_{ee} + ((c + d)s_{23} + 2s_{23}^2 e)M_{e\mu} + ((c + d)c_{23} + 2c_{23}^2 f)M_{e\tau}, \\
M_{\mu\tau} &= (a - b \cos 2\theta_{23})M_{ee} + ((d - c)s_{23} - 2s_{23}^2 e)M_{e\mu} + ((d - c)c_{23} - 2c_{23}^2 f)M_{e\tau}, \\
M_{\tau\tau} &= -b \sin 2\theta_{23}M_{ee} - (s_{23} \tan 2\theta_{23}c + e)M_{e\mu} - (c_{23} \tan 2\theta_{23}c - f)M_{e\tau}.
\end{aligned}$$

where

$$\begin{aligned}
c_{ij} &\equiv \cos \theta_{ij}, \\
s_{ij} &\equiv \sin \theta_{ij}, \\
a &= \frac{1}{2}(1 + e^{-2i\delta}), \\
b &= \frac{1}{2}(1 - e^{-2i\delta}), \\
c &= -\frac{1}{2} \cos 2\theta_{23}(e^{-i\delta} \cot 2\theta_{13} - e^{i\delta} s_{13} c_{13}^{-1}), \\
d &= e^{-i\delta} \cot 2\theta_{23} - \frac{1}{2} e^{i\delta} s_{13} c_{13}^{-1}, \\
e &= c_{23}(\cot 2\theta_{12} \sec \theta_{13} - e^{-i\delta} \csc 2\theta_{23} s_{13} c_{13}^{-1}), \\
f &= s_{23}(\cot 2\theta_{12} \sec \theta_{13} - e^{-i\delta} \csc 2\theta_{23} s_{13} c_{13}^{-1}),
\end{aligned}$$

($i, j = 1, 2, 3; i < j$) and neutrino mass eigenvalue as

$$m_{1,2,3} = f(M_{ee}, M_{e\mu}, M_{e\tau}, \theta_{12}, \theta_{23}, \theta_{13}, \delta, \alpha_2, \alpha_3). \quad (21)$$

We are interested in lepton number violating ($0\nu\beta\beta$) decay, which also confirms the Majorana nature of neutrinos. Every non-zero element of neutrino mass matrix can be written as proportional to effective Majorana mass M_{ee} as [40, 41]

$$M_{\alpha\beta} = f_{\alpha\beta}(\theta_{12}, \theta_{23}, \theta_{13}, \delta)M_{ee}, \quad (22)$$

where ($\alpha, \beta = e, \mu, \tau$).

In later study, using Eqn. (22), we identify nine hybrid textures. From literature we find out of these nine only six reproduce low energy phenomenology [31]. Now, we use Eqns. (4) and (24) in Eqn. (22) to incorporate dark matter and $0\nu\beta\beta$ decay in our study. Finally, by using the current experimental bound on relic density of dark matter we find only five hybrid textures which successfully account for the dark matter and $0\nu\beta\beta$ decay [30]. These five hybrid textures are as shown below

$$\begin{aligned}
G_1 &: \begin{pmatrix} M_{ee} & \Delta & \Delta \\ - & 0 & M_{\mu\tau} \\ - & - & M_{\tau\tau} \end{pmatrix}, & G_2 &: \begin{pmatrix} M_{ee} & 0 & M_{e\tau} \\ - & \Delta & \Delta \\ - & - & M_{\tau\tau} \end{pmatrix}, & G_3 &: \begin{pmatrix} M_{ee} & 0 & M_{e\tau} \\ - & M_{\mu\mu} & \Delta \\ - & - & \Delta \end{pmatrix}, \\
G_4 &: \begin{pmatrix} M_{ee} & M_{e\mu} & 0 \\ - & \Delta & \Delta \\ - & - & M_{\tau\tau} \end{pmatrix}, & G_5 &: \begin{pmatrix} M_{ee} & M_{e\mu} & 0 \\ - & M_{\mu\mu} & \Delta \\ - & - & \Delta \end{pmatrix},
\end{aligned}$$

where Δ represents the equal elements. In general, the elements of neutrino mass matrix for each texture is written as

$$M_{\alpha\beta} = f_{\alpha\beta}^{\mathcal{X}}(\theta_{12}, \theta_{23}, \theta_{13}, \delta) M_{ee}, \quad (23)$$

where $(\alpha, \beta = e, \mu, \tau)$ and $\mathcal{X} = G_{1\dots 5}$. The constraining equations for each hybrid texture is given in Table 1 and the corresponding expression for the coefficients $f_{\alpha\beta}^{\mathcal{X}}$ are given in Eqns. (24-28).

Texture	Constraining Equations
G_1	$Y_{e1}^2 \Lambda_1 + Y_{e2}^2 \Lambda_2 + Y_{e3}^2 \Lambda_3 = M_{ee}$
	$Y_{e1} Y_{\mu 1} \Lambda_1 + Y_{e2} Y_{\mu 2} \Lambda_2 + Y_{e3} Y_{\mu 3} \Lambda_3 = f_{e\mu}^{G_1} M_{ee}$
	$Y_{e1} Y_{\tau 1} \Lambda_1 + Y_{e2} Y_{\tau 2} \Lambda_2 + Y_{e3} Y_{\tau 3} \Lambda_3 = f_{e\tau}^{G_1} M_{ee}$
	$Y_{\mu 1}^2 \Lambda_1 + Y_{\mu 2}^2 \Lambda_2 + Y_{\mu 3}^2 \Lambda_3 = 0$
	$Y_{\mu 1} Y_{\tau 1} \Lambda_1 + Y_{\mu 2} Y_{\tau 2} \Lambda_2 + Y_{\mu 3} Y_{\tau 3} \Lambda_3 = f_{\mu\tau}^{G_1} M_{ee}$
	$Y_{\tau 1}^2 \Lambda_1 + Y_{\tau 2}^2 \Lambda_2 + Y_{\tau 3}^2 \Lambda_3 = f_{\tau\tau}^{G_1} M_{ee}$
G_2	$Y_{e1}^2 \Lambda_1 + Y_{e2}^2 \Lambda_2 + Y_{e3}^2 \Lambda_3 = M_{ee}$
	$Y_{e1} Y_{\mu 1} \Lambda_1 + Y_{e2} Y_{\mu 2} \Lambda_2 + Y_{e3} Y_{\mu 3} \Lambda_3 = 0$
	$Y_{e1} Y_{\tau 1} \Lambda_1 + Y_{e2} Y_{\tau 2} \Lambda_2 + Y_{e3} Y_{\tau 3} \Lambda_3 = f_{e\tau}^{G_2} M_{ee}$
	$Y_{\mu 1}^2 \Lambda_1 + Y_{\mu 2}^2 \Lambda_2 + Y_{\mu 3}^2 \Lambda_3 = f_{\mu\mu}^{G_2} M_{ee}$
	$Y_{\mu 1} Y_{\tau 1} \Lambda_1 + Y_{\mu 2} Y_{\tau 2} \Lambda_2 + Y_{\mu 3} Y_{\tau 3} \Lambda_3 = f_{\mu\tau}^{G_2} M_{ee}$
	$Y_{\tau 1}^2 \Lambda_1 + Y_{\tau 2}^2 \Lambda_2 + Y_{\tau 3}^2 \Lambda_3 = f_{\tau\tau}^{G_2} M_{ee}$
G_3	$Y_{e1}^2 \Lambda_1 + Y_{e2}^2 \Lambda_2 + Y_{e3}^2 \Lambda_3 = M_{ee}$
	$Y_{e1} Y_{\mu 1} \Lambda_1 + Y_{e2} Y_{\mu 2} \Lambda_2 + Y_{e3} Y_{\mu 3} \Lambda_3 = 0$
	$Y_{e1} Y_{\tau 1} \Lambda_1 + Y_{e2} Y_{\tau 2} \Lambda_2 + Y_{e3} Y_{\tau 3} \Lambda_3 = f_{e\tau}^{G_3} M_{ee}$
	$Y_{\mu 1}^2 \Lambda_1 + Y_{\mu 2}^2 \Lambda_2 + Y_{\mu 3}^2 \Lambda_3 = f_{\mu\mu}^{G_3} M_{ee}$
	$Y_{\mu 1} Y_{\tau 1} \Lambda_1 + Y_{\mu 2} Y_{\tau 2} \Lambda_2 + Y_{\mu 3} Y_{\tau 3} \Lambda_3 = f_{\mu\tau}^{G_3} M_{ee}$
	$Y_{\tau 1}^2 \Lambda_1 + Y_{\tau 2}^2 \Lambda_2 + Y_{\tau 3}^2 \Lambda_3 = f_{\tau\tau}^{G_3} M_{ee}$
G_4	$Y_{e1}^2 \Lambda_1 + Y_{e2}^2 \Lambda_2 + Y_{e3}^2 \Lambda_3 = M_{ee}$
	$Y_{e1} Y_{\mu 1} \Lambda_1 + Y_{e2} Y_{\mu 2} \Lambda_2 + Y_{e3} Y_{\mu 3} \Lambda_3 = f_{e\mu}^{G_4} M_{ee}$
	$Y_{e1} Y_{\tau 1} \Lambda_1 + Y_{e2} Y_{\tau 2} \Lambda_2 + Y_{e3} Y_{\tau 3} \Lambda_3 = 0$
	$Y_{\mu 1}^2 \Lambda_1 + Y_{\mu 2}^2 \Lambda_2 + Y_{\mu 3}^2 \Lambda_3 = f_{\mu\mu}^{G_4} M_{ee}$
	$Y_{\mu 1} Y_{\tau 1} \Lambda_1 + Y_{\mu 2} Y_{\tau 2} \Lambda_2 + Y_{\mu 3} Y_{\tau 3} \Lambda_3 = f_{\mu\tau}^{G_4} M_{ee}$
	$Y_{\tau 1}^2 \Lambda_1 + Y_{\tau 2}^2 \Lambda_2 + Y_{\tau 3}^2 \Lambda_3 = f_{\tau\tau}^{G_4} M_{ee}$
G_5	$Y_{e1}^2 \Lambda_1 + Y_{e2}^2 \Lambda_2 + Y_{e3}^2 \Lambda_3 = M_{ee}$
	$Y_{e1} Y_{\mu 1} \Lambda_1 + Y_{e2} Y_{\mu 2} \Lambda_2 + Y_{e3} Y_{\mu 3} \Lambda_3 = f_{e\mu}^{G_5} M_{ee}$
	$Y_{e1} Y_{\tau 1} \Lambda_1 + Y_{e2} Y_{\tau 2} \Lambda_2 + Y_{e3} Y_{\tau 3} \Lambda_3 = 0$
	$Y_{\mu 1}^2 \Lambda_1 + Y_{\mu 2}^2 \Lambda_2 + Y_{\mu 3}^2 \Lambda_3 = f_{\mu\mu}^{G_5} M_{ee}$
	$Y_{\mu 1} Y_{\tau 1} \Lambda_1 + Y_{\mu 2} Y_{\tau 2} \Lambda_2 + Y_{\mu 3} Y_{\tau 3} \Lambda_3 = f_{\mu\tau}^{G_5} M_{ee}$
	$Y_{\tau 1}^2 \Lambda_1 + Y_{\tau 2}^2 \Lambda_2 + Y_{\tau 3}^2 \Lambda_3 = f_{\tau\tau}^{G_5} M_{ee}$

Table 1: Constraining equations relating loop factors and Yukawa couplings to the effective Majorana neutrino mass $|M_{ee}|$ for all hybrid textures $G_{1\dots 5}$.

$$\left. \begin{aligned}
f_{e\mu}^{G_1} &= \frac{\sin 2\theta_{12} \sin 2\theta_{13} (e^{2i\delta} c_{23}^2 + s_{23}^2)}{-4e^{2i\delta} L_5 (c_{23} - s_{23}) c_{23}^2 K_3 + \frac{e^{i\delta}}{\csc 2\theta_{12}} (2e^{2i\delta} c_{23}^2 K_3 + s_{23} (K_1 - \frac{2M_3}{\sin 2\theta_{12}}))}, \\
f_{\mu\tau}^{G_1} &= \frac{\sqrt{2} \cos(\frac{\pi}{4} + \theta_{23}) (-\frac{4e^{i\delta} L_5}{\sec 2\theta_{23}} + \frac{2 \sin 2\theta_{12}}{\csc 2\theta_{23}} (s_{13}^2 + e^{2i\delta} (\frac{\cos^2 \theta_{13}}{\sin 2\theta_{23}} + 1)))}{-4e^{3i\delta} L_5 (c_{23} - s_{23}) c_{23}^2 K_3 + \frac{e^{i\delta}}{\csc 2\theta_{12}} (2e^{2i\delta} c_{23}^2 K_3 + s_{23} (K_1 - \frac{2M_3}{\sin 2\theta_{12}}))}, \\
f_{\tau\tau}^{G_1} &= \frac{\sin 2\theta_{12} (\frac{2(c_{23} - s_{23})}{\csc^2 \theta_{13} \csc^2 \theta_{23}} + \frac{e^{2i\delta}}{\sec \theta_{23}} (\frac{M_3}{\sin 2\theta_{12}} + \sin 2\theta_{23}) - e^{i\delta} L_5 (L_1 - K_5))}{-4e^{3i\delta} L_5 (c_{23} - s_{23}) c_{23}^2 K_3 + \frac{e^{i\delta}}{\csc 2\theta_{12}} (2e^{2i\delta} c_{23}^2 K_3 + s_{23} (K_1 - \frac{2M_3}{\sin 2\theta_{12}}))},
\end{aligned} \right\} \quad (24)$$

$$\left. \begin{aligned}
f_{e\tau}^{G_2} &= \frac{\sin 2\theta_{12} \sin 2\theta_{13} (K_1 + e^{2i\delta} K_2)}{2e^{i\delta} \sin 2\theta_{12} (2e^{2i\delta} c_{23}^2 K_3 + s_{23} (K_4 - \sin 2\theta_{23})) + 2e^{2i\delta} L_5 (K_5 + L_1)}, \\
f_{\mu\tau}^{G_2} &= \frac{4s_{23} (e^{i\delta} c_{23} s_{12} + c_{12} s_{13} s_{23}) (e^{i\delta} c_{12} c_{23} - s_{12} s_{13} s_{23})}{2e^{i\delta} \sin 2\theta_{12} (2e^{2i\delta} c_{23}^2 K_3 + s_{23} (K_4 - \sin 2\theta_{23})) + e^{3i\delta} L_5 (K_5 + L_1)}, \\
f_{\tau\tau}^{G_2} &= \frac{\frac{(N_1 - 2K_5)}{\csc 2\theta_{12} \csc^2 \theta_{13}} + \frac{e^{2i\delta}}{\csc 2\theta_{12}} (2(\cos 3\theta_{23} + \frac{K_3 \cos 2\theta_{13}}{s_{13}^2} + e^{i\delta} L_5 (K_5 + 2N_1)) - N_1)}{2e^{i\delta} \sin 2\theta_{12} (2e^{2i\delta} c_{23}^2 K_3 + s_{23} (K_4 - \sin 2\theta_{23})) + 2e^{3i\delta} L_5 (K_5 + L_1)},
\end{aligned} \right\} \quad (25)$$

$$\left. \begin{aligned}
f_{e\tau}^{G_3} &= \frac{\sin 2\theta_{12} s_{13} ((K_1 + 2 \cos 2\theta_{23}) + e^{2i\delta} (K_2 - 2 \cos 2\theta_{23}))}{8e^{2i\delta} L_5 s_{23}^2 K_3 - e^{i\delta} \sin 2\theta_{12} (L_3 - 2K_4 s_{23}) + e^{3i\delta} \sin 2\theta_{12} s_{13}^2 (K_5 + N_1)}, \\
f_{\mu\tau}^{G_3} &= \frac{2s_{23} (e^{2i\delta} K_4 \sin 2\theta_{12} + 2 \cos^2 \theta_{23} L_4 + 2e^{i\delta} \sin 2\theta_{23} L_5)}{8e^{3i\delta} L_5 s_{23}^2 K_3 - e^{2i\delta} \sin 2\theta_{12} (L_3 - 2K_4 s_{23}) + e^{4i\delta} \sin 2\theta_{12} s_{13}^2 (K_5 + N_1)}, \\
f_{\mu\mu}^{G_3} &= \frac{\frac{2}{\csc 2\theta_{12}} (\frac{2(2c_{23} - s_{23})}{\csc \theta_{13}^2} - \frac{e^{2i\delta}}{\sec \theta_{23}} (K_4 - K_1 - \frac{2}{\csc 2\theta_{23}})) + e^{i\delta} \frac{s_{13}}{\tan 2\theta_{12}} (K_5 - 2N_1)}{8e^{3i\delta} L_5 s_{23}^2 K_3 - e^{2i\delta} \sin 2\theta_{12} (L_3 - 2K_4 s_{23}) + e^{4i\delta} \sin 2\theta_{12} s_{13}^2 (K_5 + N_1)},
\end{aligned} \right\} \quad (26)$$

$$\left. \begin{aligned}
f_{e\mu}^{G_4} &= \frac{\sin 2\theta_{12} \sin 2\theta_{13} (K_1 + e^{2i\delta} K_2)}{\frac{-8e^{2i\delta} c_{13}^2}{s_{13}^2} K_3 L_5 + \frac{2e^{i\delta}}{\csc 2\theta_{12}} (M_1 \cos 2\theta_{13} + M_2 c_{23}) + e^{3i\delta} L_4 (K_5 + L_1)}, \\
f_{\mu\tau}^{G_4} &= \frac{2c_{23} (e^{2i\delta} M_3 + 2M_4 - 2e^{i\delta} L_5 \sin 2\theta_{23})}{\frac{-8e^{3i\delta} c_{13}^2}{s_{13}^2} K_3 L_5 + \frac{2e^{2i\delta}}{\csc 2\theta_{12}} (M_1 \cos 2\theta_{13} + M_2 c_{23}) + e^{4i\delta} L_4 (K_5 + L_1)}, \\
f_{\tau\tau}^{G_4} &= \frac{2(\sin 2\theta_{12} (-2c_{23}^2 s_{13}^2 M_1 + e^{2i\delta} N_2 - e^{i\delta} L_5 (2L_2 + L_1)))}{\frac{-8e^{3i\delta} c_{13}^2}{s_{13}^2} K_3 L_5 + \frac{2e^{2i\delta}}{\csc 2\theta_{12}} (M_1 \cos 2\theta_{13} + M_2 c_{23}) + e^{4i\delta} L_4 (K_5 + L_1)},
\end{aligned} \right\} \quad (27)$$

$$\left. \begin{aligned}
f_{e\mu}^{G_5} &= \frac{\sin 2\theta_{12} s_{13} ((K_1 + 2 \cos 2\theta_{23}) + e^{2i\delta} (K_1 + 2 \sin 2\theta_{23}))}{\frac{4e^{3i\delta} M_4 K_3}{s_{13}^2} - 2e^{i\delta} c_{23} \sin 2\theta_{12} (K_2 - c_{13}^2) - 2e^{2i\delta} L_5 (K_5 + L_1)}, \\
f_{\mu\mu}^{G_5} &= \frac{16e^{i\delta} L_5 (L_2 - \frac{c_{23}}{\csc 2\theta_{23}}) - \frac{4e^{2i\delta}}{\csc 2\theta_{12}} (\frac{e^{-2i\delta} N_3}{\csc \theta_{13}^2} - (L_2 - \frac{2 \cos 2\theta_{13} K_3}{s_{13}^2} + \frac{2}{\csc 3\theta_{23}}))}{\frac{16e^{4i\delta} M_4 K_3}{s_{13}^2} + 8e^{2i\delta} c_{23} \sin 2\theta_{12} (K_2 - c_{13}^2) - 8e^{3i\delta} L_5 (K_5 + L_1)}, \\
f_{\mu\tau}^{G_5} &= \frac{4c_{23} (c_{23} s_{12} s_{13} + e^{i\delta} \frac{\sin 2\theta_{12}}{2}) (-c_{12} c_{23} s_{13} + e^{i\delta} s_{12} s_{23})}{\frac{2e^{4i\delta} M_4 K_3}{s_{13}^2} - e^{2i\delta} c_{23} \sin 2\theta_{12} (K_2 - c_{13}^2) - 3e^{3i\delta} L_5 (K_5 + L_1)},
\end{aligned} \right\} \quad (28)$$

where

$$\left. \begin{aligned}
K_1 &= 1 - \cos 2\theta_{23} - \sin 2\theta_{23}, \\
K_2 &= 1 + \cos 2\theta_{23} + \sin 2\theta_{23}, \\
K_3 &= s_{13}^2(c_{23} + s_{23}), \\
K_4 &= \cos 2\theta_{13} + \cos 2\theta_{23}, \\
K_5 &= c_{23} - \cos 3\theta_{23}, \\
L_1 &= s_{23} + \sin 3\theta_{23}, \\
L_2 &= c_{23} + \cos 3\theta_{23}, \\
L_3 &= (-1 + 4 \cos 2\theta_{13}) \cos 2\theta_{23} + \cos 3\theta_{23}, \\
L_4 &= \sin 2\theta_{12} s_{13}^2, \\
L_5 &= \cos 2\theta_{12} s_{13}, \\
M_1 &= c_{23} - 2s_{23}, \\
M_2 &= -\cos 2\theta_{23} + \sin 2\theta_{23}, \\
M_3 &= \sin 2\theta_{12} (\cos 2\theta_{13} - \cos 2\theta_{23}), \\
M_4 &= \sin 2\theta_{12} s_{13}^2 s_{23}^2, \\
N_1 &= -s_{23} + \sin 3\theta_{23}, \\
N_2 &= s_{23} (2(\cos 2\theta_{23} + s_{13}^2) + \sin 2\theta_{23}), \\
N_3 &= \cos 3\theta_{23} + c_{23} (-1 + 4 \sin 2\theta_{23}),
\end{aligned} \right\} \quad (29)$$

Mixing angles	bfp $\pm 1\sigma$	3σ range
$\theta_{12}/^\circ$	$33.82^{+0.78}_{-0.76}$	$31.61 \rightarrow 36.27$
$\theta_{23}/^\circ$	$49.6^{+1.0}_{-1.2}$	$40.3 \rightarrow 52.4$
$\theta_{13}/^\circ$	$8.61^{+0.13}_{-0.13}$	$8.22 \rightarrow 8.99$
$\delta/^\circ$	215^{+40}_{-29}	$125 \rightarrow 392$

Table 2: Global fit data of neutrino mixing angles and CP phase δ [42].

Clearly, f_{ee} coefficients for all these hybrid textures are unity. All these coefficients $f_{\alpha\beta}^{\mathcal{X}}$ are calculated by randomly generating the mixing angles and CP phase within their allowed range using the data given in Table 2 [42].

4 Lepton Asymmetry

Leptogenesis offers a minimal framework to comprehend the dynamical origin of baryon asymmetry of universe, even though the origins of this baryon asymmetry may be completely distinct. In our universe, which most likely started off as baryon symmetric, there are three fundamental conditions called Sakharov's conditions, that must be met for the dynamical generation of this asymmetry. These three conditions are (i) baryon number violation, (ii) C and CP , violation and (iii) departure from thermal equilibrium.

In our work, we take into account the out-of-equilibrium decay of the heavy right-handed neutrinos, the eminent method to find the lepton asymmetry [43–48]. The lepton asymmetry due to the decay of the right-handed neutrinos into Higgs and leptons is given by

$$\epsilon_{N_k} = \sum_i \frac{\Gamma(N_k \rightarrow L_i + H^\dagger) - \Gamma(N_k \rightarrow \bar{L}_i + H)}{\Gamma(N_k \rightarrow L_i + H^\dagger) + \Gamma(N_k \rightarrow \bar{L}_i + H)} \quad (30)$$

At very high temperatures ($T \geq 10^{12} GeV$), all charged flavours are out of equilibrium and behave similarly, resulting in the unflavored regime. However, at temperatures $T < 10^{12} GeV$ ($T < 10^9 GeV$), tau (muon) Yukawa couplings enter equilibrium, and flavour effects become important in the calculation of lepton asymmetry [49–52]. The temperature ranges $10^9 GeV < T < 10^{12} GeV$ and $T < 10^9 GeV$ correspond to two and three flavour leptogenesis regimes, respectively. We assume a hierarchical spectrum for the heavy right handed neutrino, $M_1 \leq M_2 < M_3$. As a result, the source of lepton asymmetry is the decay of the lightest right handed neutrino N_1 . The asymmetry caused by the decay of N_1 is calculated as [53]

$$\begin{aligned} \epsilon_1^\alpha &= \frac{1}{8\pi} \frac{1}{[Y^\dagger Y]_{11}} \sum_{j=2,3} Im[Y_{\alpha 1}^\dagger (Y^\dagger Y)_{1j}^2 Y_{\alpha j}^\dagger] g(x_j) \\ &+ \frac{1}{8\pi} \frac{1}{[Y^\dagger Y]_{11}} \sum_{j=2,3} Im[Y_{\alpha 1}^\dagger (Y^\dagger Y)_{j1}^2 Y_{\alpha j}^\dagger] \frac{1}{1-x_j} \end{aligned} \quad (31)$$

where

$$g(x) = \sqrt{x} \left(1 + \frac{1}{1-x} - (1+x) \ln \frac{1+x}{x} \right), \text{ and } x_j = M_j^2/M_1^2.$$

When summed over all flavors ($\alpha = e, \mu, \tau$), the second term in ϵ_1^α vanishes and sum over all flavors is given by

$$\epsilon_1 = \frac{1}{8\pi} \frac{1}{[Y^\dagger Y]_{11}} \sum_{j=2,3} Im[(Y^\dagger Y)_{1j}^2] g(x_j) \quad (32)$$

The lepton asymmetry through electroweak sphaleron process gives rise to baryon asymmetry is given by [54]

$$Y_B = ck \frac{\epsilon_1}{g_*} \quad (33)$$

where c is the fraction of lepton asymmetry converted to baryon asymmetry, which is approximately equal to -0.55, and k is the dilution factor due to washout processes that erase the produced asymmetry, which can be parameterized as [55–57]

$$\begin{aligned} -k &\approx \sqrt{0.1K} \exp[-4/(3(0.1K)^{0.25})], \text{ for } K \geq 10^6 \\ &\approx \frac{0.3}{K(\ln K)^{0.6}}, \text{ for } 10 \leq K \leq 10^6 \\ &\approx \frac{1}{2\sqrt{K^2+9}}, \text{ for } 0 \leq K \leq 10, \end{aligned} \quad (34)$$

where K is given by

$$K = \frac{\Gamma_1}{H(T=M_1)} = \frac{(Y^\dagger Y)_{11} M_1}{8\pi v^2} \frac{M_{pl}}{1.66\sqrt{g_*} M_1^2}. \quad (35)$$

Here Γ_1 is the decay width of N_1 and $H(T = M1)$ is the Hubble constant at temperature ($T = M1$). The factor g_* is the effective number of relativistic degrees of freedom at ($T = M1$) and is approximately equal to 110.

The two flavor and three flavor leptogenesis is given by

$$Y_B^{2flavor} = \frac{-12}{37g^*} \left[\epsilon_2 \eta \left(\frac{417}{589} \tilde{m}_2 \right) + \epsilon_1^\tau \eta \left(\frac{390}{589} \tilde{m}_\tau \right) \right] \quad (36)$$

$$Y_B^{3flavor} = \frac{-12}{37g^*} \left[\epsilon_1^e \eta \left(\frac{151}{179} \tilde{m}_e \right) + \epsilon_1^\mu \eta \left(\frac{344}{537} \tilde{m}_\mu \right) + \epsilon_1^\tau \eta \left(\frac{344}{537} \tilde{m}_\tau \right) \right] \quad (37)$$

Where

$$\left. \begin{aligned} \epsilon_2 &= \epsilon_1^e + \epsilon_1^\mu, \\ \tilde{m}_2 &= \tilde{m}_e + \tilde{m}_\mu, \\ \tilde{m}_\alpha &= \frac{v^2(Y^\dagger Y)_{\alpha 1}}{M_1}, \end{aligned} \right\} \quad (38)$$

The function η is given by

$$\eta(\tilde{m}_\alpha) = \left[\left(\frac{\tilde{m}_\alpha}{8.25 \times 10^{-3} eV} \right)^{-1} + \left(\frac{0.2 \times 10^{-3} eV}{\tilde{m}_\alpha} \right)^{-1.16} \right]^{-1} \quad (39)$$

5 Numerical analysis and discussion

In the preceding sections, we first set the framework to find the branching ratio for the flavor violating process $Br(\mu \rightarrow e\gamma)$, and relic density of dark matter (Ωh^2). We also discuss the expressions which relates dark matter and neutrinoless double beta decay. Then, finally in the last section we discuss the framework to calculate the lepton asymmetry and baryon asymmetry of universe.

We calculate the loop functions Λ_k for each texture using Eqn.(5) by randomly generating quartic coupling λ , lightest right-handed neutrino mass M_1 with in their specified ranges given in Table 3. As stated before, we assume mass hierarchy $M_1 \leq M_2 < M_3$ and $m_0 \gtrsim M_1$ in the calculation of λ_k . Substituting Λ_k 's and randomly varying the diagonal Yukawa couplings ($Y_{e1}, Y_{\mu 2}, Y_{\tau 3}$) on the left-hand side and $|M_{ee}|$ in the range (0 – 0.25) eV on the right-hand side of constraining equations given in Table 1, we calculate the off-diagonal Yukawa couplings and constraining them in the range 0 - 1.5. Furthermore, the numerical analysis imposes bounds on the LFV process $\mu \rightarrow e\gamma$ i.e., $Br(\mu \rightarrow e\gamma) \leq 4.2 \times 10^{-13}$ and on dark matter mass M_1 given in Table 4 [58].

The data obtained in this manner met all of the requirements for the simultaneous validation of dark matter and neutrinoless double beta decay. Now, we use these masses of the right handed neutrinos and Yukawa couplings in Eqns. (32) and (34) to calculate the lepton asymmetry ϵ_1 and dilution factor k which then put in Eqn. (33) to get the final baryon asymmetry.

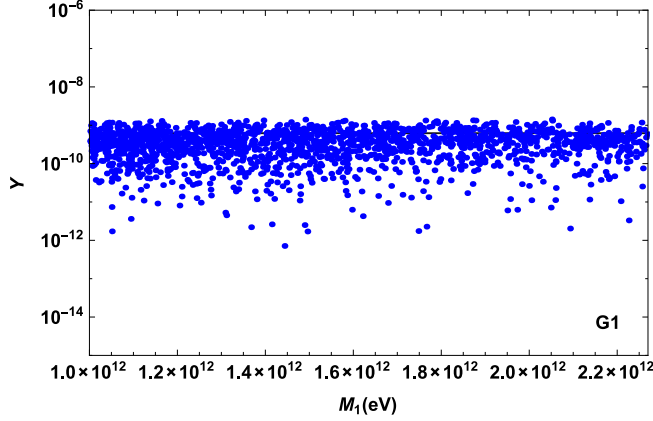


Figure 1: Correlation between baryon asymmetry of universe Y and DM mass M_1 for texture G_1 . The horizontal line is the observed value of baryon asymmetry of universe $Y = (6.04 \pm 0.08) \times 10^{-10}$ [1].

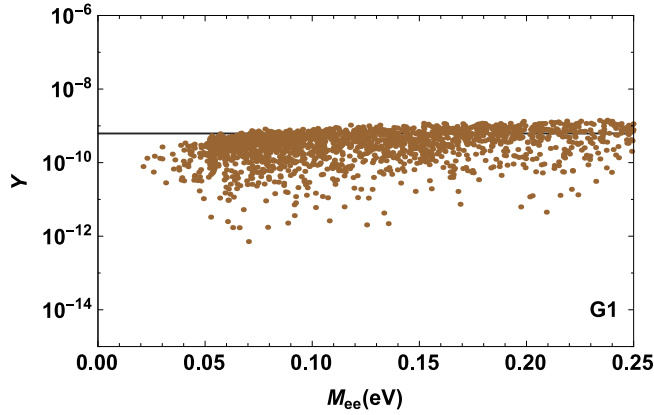


Figure 2: Correlation between baryon asymmetry of universe Y with effective Majorana mass $|M_{ee}|$ for texture G_1 . The horizontal line is the observed value of baryon asymmetry of universe $Y = (6.04 \pm 0.08) \times 10^{-10}$ [1].

Parameter	Range
λ	$(3 - 4) \times 10^{-9}$
$Y_{e1}, Y_{\mu2}, Y_{\tau3}$	0 - 1.5
M_1	$\mathcal{O}(TeV)$

Table 3: Ranges of parameters used in the numerical analysis.

We find the correlation plots of baryon asymmetry of universe Y with Dark matter mass M_1 , effective Majorana mass $|M_{ee}|$ and relic density of DM as shown in Fig. 1 to Fig. 6. We plot baryon asymmetry of universe with relic density of DM to check the simultaneity of DM and BAU by considering 4 TeV as upper bound on DM mass. The horizontal lines in the given correlation plots corresponding to the observed value of the baryon asymmetry of the universe $Y = (6.04 \pm 0.08) \times 10^{-10}$ and the vertical line in Fig. 3 and Fig. 6 is the observed value of relic density of DM $\Omega h^2 = 0.120 \pm 0.001$ [1]. Fig. 1 shows the correlation between baryon asymmetry of universe Y and dark matter mass M_1 for the hybrid texture G_1 . The plot shows that

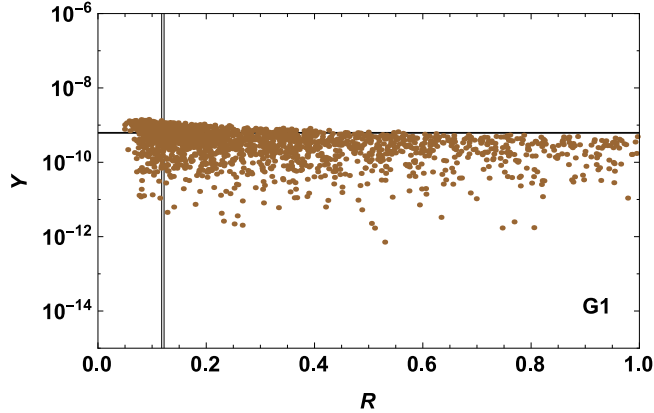


Figure 3: Correlation between baryon asymmetry of universe Y and Relic density of DM (Ωh^2) for the texture G_1 . The vertical line is the observed value of relic density of DM $\Omega h^2 = 0.120 \pm 0.001$ and the horizontal line is the observed value of baryon asymmetry of universe $Y = (6.04 \pm 0.08) \times 10^{-10}$ [1].

the texture G_1 produce successful baryogenesis through leptogenesis for the allowed range of DM mass i.e. $1TeV$ to $2.27TeV$. Similarly Fig. 4 shows the correlation plots between Y and M_1 for the hybrid textures $G_{2,..5}$ and we find that these textures produce successful leptogenesis as they satisfy the baryon asymmetry seen by Planck experiment. Fig. 2 shows the correlation between baryon asymmetry of universe Y with effective Majorana mass $|M_{ee}|$ for texture G_1 which successfully produce correct baryon asymmetry for effective Majorana mass $\geq 0.052 eV$. Fig. 5 shows the correlation plots for baryon asymmetry of universe Y verses effective Majorana mass $|M_{ee}|$ for textures $G_{2,..5}$. It is clear from the Fig. 5 that these textures produce correct baryon asymmetry of universe $Y = (6.04 \pm 0.08) \times 10^{-10}$ [1] and gives a lower bounds on the effective Majorana mass $|M_{ee}|$ as shown in Table 4.

6 Conclusions

We investigate the leptogenesis, dark matter and neutrinoless double beta decay in the hybrid textures of neutrino mass matrix at one loop level. There are five hybrid textures which simultaneously accounts for the DM and neutrinoless double beta decay. We extend this idea to the simultaneous study of leptogenesis DM and neutrinoless double beta decay. We use the neutrino oscillation data and find the Yukawa couplings and use them to find the relic density of DM (Ωh^2) and baryon asymmetry of universe. The correlation plots for these quantities shown in Fig. 1, Fig. 2, Fig. 4 and Fig. 5. Fig. 1 and Fig. 4 show the predicted parameter space between baryon asymmetry of universe Y and DM mass M_1 for the textures $G_{1,..5}$. Therefore, from these figures we find that all these textures $G_{1,..5}$ produce correct baryon asymmetry $Y = (6.04 \pm 0.08) \times 10^{-10}$ [1]. Fig. 2 and Fig. 5 show the predicted parameter space for the baryon asymmetry of universe Y and effective Majorana mass $|M_{ee}|$ for the textures $G_{1,..5}$. From these figures we find that the textures $G_{1,..5}$ produce correct baryon asymmetry and give lower bound to the effective Majorana mass $|M_{ee}|$. The most interesting plots are the correlation plots shown in Fig. 3 and Fig. 6 between

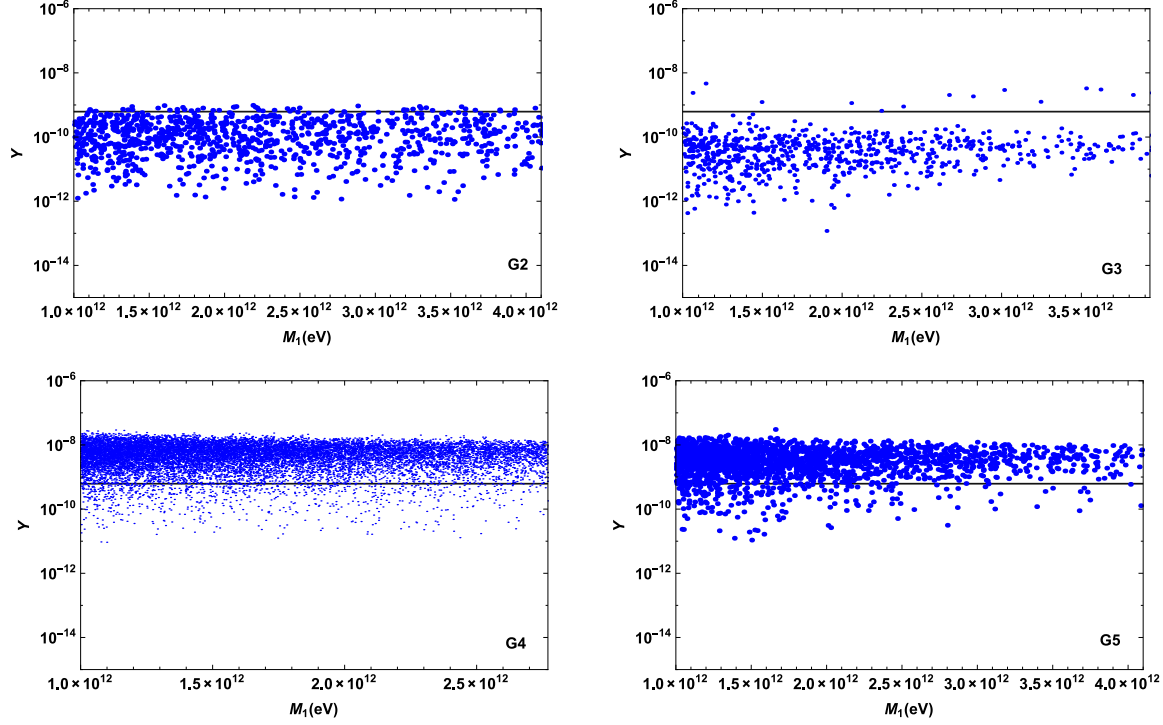


Figure 4: Correlation between baryon asymmetry of universe Y and DM mass M_1 for textures $G_{2,\dots,5}$. The horizontal line is the observed value of baryon asymmetry of universe $Y = (6.04 \pm 0.08) \times 10^{-10}$ [1].

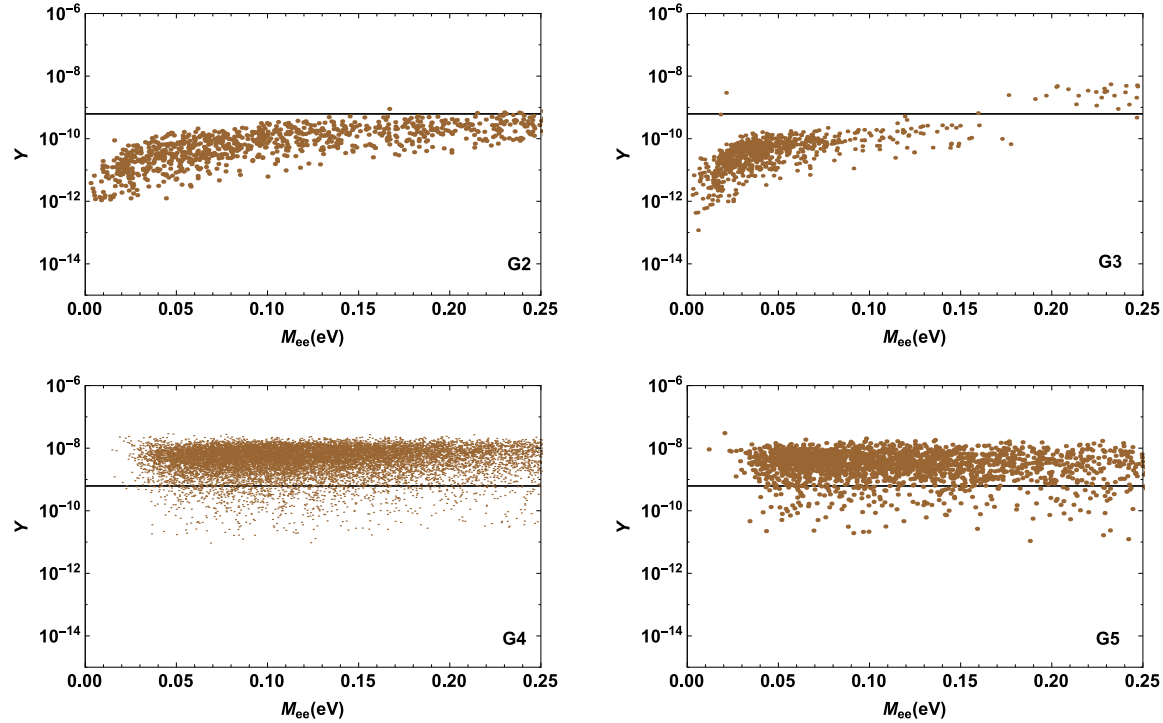


Figure 5: Correlation between baryon asymmetry of universe Y with effective Majorana mass $|M_{ee}|$ for textures $G_{2,\dots,5}$. The horizontal line is the observed value of baryon asymmetry of universe $Y = (6.04 \pm 0.08) \times 10^{-10}$ [1].

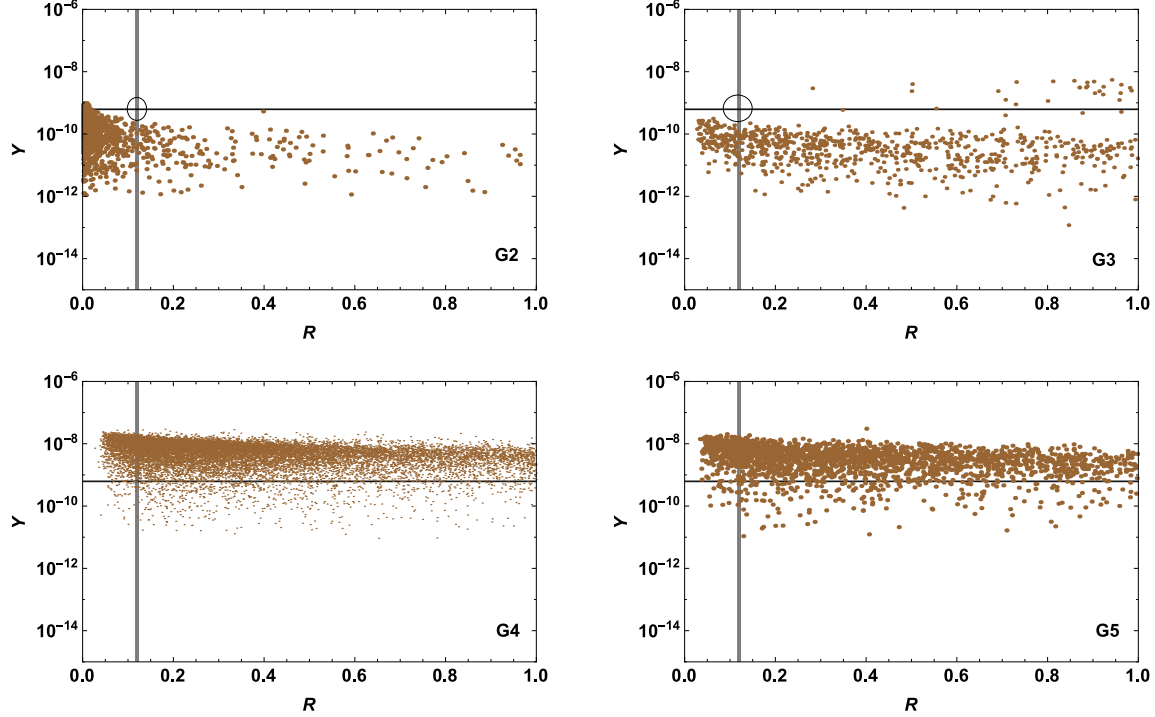


Figure 6: Correlation between baryon asymmetry of universe Y and Relic density of DM (Ωh^2). The vertical line is the observed value of relic density of DM $\Omega h^2 = 0.120 \pm 0.001$ and the horizontal line is the observed value of baryon asymmetry of universe $Y = (6.04 \pm 0.08) \times 10^{-10}$ [1].

baryon asymmetry of universe (Y) and relic density of dark matter (R). These plots are of more interest because confirm the simultaneity of the baryon asymmetry of universe Y and dark matter M_1 with the determination of R . The textures G_2 and G_3 have been found to either satisfy the relic density bound $\Omega h^2 = 0.120 \pm 0.001$ or the bound on baryon asymmetry of the universe $Y = (6.04 \pm 0.08) \times 10^{-10}$ shown in the first row of Fig. 6 as there is no point satisfying both bounds, i.e. on or around the intersection of both bounds marked by small circles. Therefore, these textures (i.e. G_2 and G_3) do not show the simultaneity of the BAU and DM hence, discarded. Therefore, it has been found that out of five textures $G_{1...5}$ only textures G_1 , G_4 and G_5 simultaneously account for the leptogenesis, dark matter and neutrinoless double beta decay. Another interesting fact to note that is interesting to note Fig. 2 and Fig. 5 give lower bound to the $|M_{ee}|$ shown in Table 4. More evidence for or against the theories can be provided by the observation of $|M_{ee}|$ in past, present, and future neutrinoless double beta decay experiments [59–63]. These tests can explore smaller values of $|M_{ee}|$ with previously unheard-of sensitivity. The experiments e.g. SuperNEMO, KamLAND-Zen, NEXT, and nEXO (5 year) have sensitivity reaches of 0.05 eV, 0.045 eV, 0.03 eV, and 0.015 eV, respectively [59–63].

Texture	$M_1(TeV)$	$ M_{ee} (eV)$	Leptogenesis
G_1	≤ 2.27	≥ 0.052	✓
G_2	≤ 5.31	disallowed by the observed value of relic density of DM(Ωh^2) and BAU (Y)	
G_3	≤ 3.93	disallowed by the observed value of relic density of DM(Ωh^2) and BAU (Y)	
G_4	≤ 2.77	≥ 0.021	✓
G_5	≤ 4.10	≥ 0.034	✓

Table 4: Ranges considered for the DM mass and bounds on effective Majorana mass $|M_{ee}|$ for allowed hybrid textures.

Acknowledgments

Ankush acknowledges the financial support provided by the University Grants Commission, Government of India vide registration number 201819-NFO-2018-19-OBC-HIM-75542. R. Verma acknowledges the financial support provided by the Central University of Himachal Pradesh. B. C. Chauhan is thankful to the Inter University Centre for Astronomy and Astrophysics (IUCAA) for providing necessary facilities during the completion of this work.

References

- [1] N. Aghanim *et al.* [Planck], *Astron. Astrophys.* **641**, A6 (2020).
- [2] R. Verma, Ankush and B. C. Chauhan, [arXiv:2302.09282 [hep-ph]].
- [3] R. Verma, M. Kashav, S. Verma and B. C. Chauhan, *PTEP* **2021**, no.12, 123B01 (2021).
- [4] E. Ma, *Phys. Rev. D* **73**, 077301 (2006).
- [5] P. Minkowski, *Phys. Lett. B* **67**, 421 (1977).
- [6] R. N. Mohapatra and G. Senjanovic, *Phys. Rev. Lett.* **44**, 912 (1980).
- [7] T. Yanagida, *Conf. Proc. C* **7902131**, 95 (1979).
- [8] S. L. Glashow, *NATO Sci. Ser. B* **61**, 687 (1980).
- [9]] M. Gell-Mann, P. Ramond, and R. Slansky, *Conf. Proc. C* **790927**, 315 (1979).
- [10] E. Ma, *Phys. Rev. Lett.* **81**, 1171 (1998).
- [11] A. Zee, *Phys. Lett. B* **93**, 389 (1980).
- [12] E. Ma and M. Raidal, *Phys. Rev. Lett.* **87**, 011802 (2001).
- [13] J. Kubo, E. Ma and D. Suematsu, *Phys. Lett. B* **642**, 18 (2006).
- [14] T. Hambye, K. Kannike, E. Ma and M. Raidal, *Phys. Rev. D* **75**, 095003 (2007).
- [15] Y. Farzan, *Phys. Rev. D* **80**, 073009 (2009).

- [16] E. Ma and U. Sarkar, Phys. Lett. B **653**, 288 (2007).
- [17] E. Ma, Phys. Lett. B **662**, 49 (2008).
- [18] Y. Kajiyama, H. Okada and K. Yagyu, Nucl. Phys. B **874**, 198 (2013).
- [19] M. Aoki, J. Kubo and H. Takano, Phys. Rev. D **87**, 116001 (2013).
- [20] Y. Kajiyama, H. Okada and T. Toma, Phys. Rev. D **88**, 015029 (2013).
- [21] L. M. Krauss, S. Nasri and M. Trodden, Phys. Rev. D **67**, 085002 (2003).
- [22] M. Aoki, S. Kanemura and O. Seto, Phys. Rev. Lett. **102**, 051805 (2009).
- [23] M. Gustafsson, J. M. No and M. A. Rivera, Phys. Rev. Lett. **110**, 211802 (2013).
- [24] A. Ahriche, C. S. Chen, K. L. McDonald and S. Nasri, Phys. Rev. D **90**, 015024 (2014).
- [25] A. Ahriche, K. L. McDonald and S. Nasri, JHEP **10**, 167 (2014).
- [26] T. Nomura and H. Okada, Phys. Lett. B **770**, 307 (2017).
- [27] F. Bonnet, M. Hirsch, T. Ota and W. Winter, JHEP **07**, 153 (2012).
- [28] T. Kitabayashi, Phys. Rev. D **98**, 083011 (2018).
- [29] T. Kitabayashi, S. Ohkawa and M. Yasuè, Int. J. Mod. Phys. A **32**, 1750186 (2017).
- [30] Ankush, M. Kashav, S. Verma and B. C. Chauhan, Phys. Lett. B **824**, 136796 (2022).
- [31] S. Dev, S. Verma and S. Gupta, Phys. Lett. B **687**, 53 (2010).
- [32] S. Kaneko, H. Sawanaka and M. Tanimato, JHEP **0508**, 073 (2005).
- [33] S. Goswami, S. Khan and A. Watanabe, Phys. Lett. B **693**, 249 (2010).
- [34] J. Y. Liu and S. Zhou, Phys. Rev. D **87**, 093010 (2013).
- [35] R. Kalita and D. Borah, Int. J. Mod. Phys. A **31**, 1650008 (2016).
- [36] A. Vicente and C. E. Yaguna, JHEP **02**, 144 (2015)
- [37] K. Griest and D. Seckel, Phys. Rev. D **43**, 3191 (1991).
- [38] D. Suematsu, T. Toma and T. Yoshida, Phys. Rev. D **79**, 093004 (2009).
- [39] E. W. Kolb and M. S. Turner, Front. Phys. **69**, 1-547 (1990).
- [40] T. Kitabayashi and M. Yasuè, Phys. Rev. D **93**, 053012 (2016).
- [41] T. Kitabayashi and M. Yasuè, Int. J. Mod. Phys. A **31**, 1650043 (2016).

- [42] I. Esteban, M. C. Gonzalez-Garcia, A. Hernandez-Cabezudo, M. Maltoni and T. Schwetz, JHEP **01**, 106 (2019).
- [43] N. Gautam and M. K. Das, Phys. Lett. B **833**, 137302 (2022).
- [44] S. Weinberg, Phys. Rev. Lett. **42**, 850-853 (1979).
- [45] E. W. Kolb and S. Wolfram, Nucl. Phys. B **172**, 224 (1980).
- [46] T. Hugle, M. Platscher and K. Schmitz, Phys. Rev. D **98**, no.2, 023020 (2018).
- [47] D. Borah, P. S. B. Dev and A. Kumar, Phys. Rev. D **99**, no.5, 055012 (2019).
- [48] J. Racker, JCAP **03**, 025 (2014).
- [49] R. Barbieri, P. Creminelli, A. Strumia and N. Tetradis, Nucl. Phys. B **575**, 61-77 (2000).
- [50] A. Abada, S. Davidson, F. X. Josse-Michaux, M. Losada and A. Riotto, JCAP **04**, 004 (2006).
- [51] A. Abada, S. Davidson, A. Ibarra, F. X. Josse-Michaux, M. Losada and A. Riotto, JHEP **09**, 010 (2006).
- [52] P. S. Bhupal Dev, P. Millington, A. Pilaftsis and D. Teresi, Nucl. Phys. B **886**, 569-664 (2014).
- [53] A. S. Joshipura, E. A. Paschos and W. Rodejohann, Nucl. Phys. B **611**, 227-238 (2001).
- [54] V. Kuzmin, V. Rubakov, and M. Shaposhnikov, Phys. Lett. B **155**, 36 (1985).
- [55] E. W. Kolb and M. S. Turner, Front. Phys. **69**, 1 (1990).
- [56] A. Pilaftsis, Int. J. Mod. Phys. A **14**, 1811-1858 (1999).
- [57] M. Flanz and E. A. Paschos, Phys. Rev. D **58**, 113009 (1998).
- [58] A. M. Baldini *et al.*, Eur. Phys. J. C **76**, 434 (2016).
- [59] A. S. Barabash, J. Phys. Conf. Ser. **375**, 042012 (2012).
- [60] A. Gando *et al.*, Phys. Rev. Lett. **117**, no.8, 082503 (2016).
- [61] J. J. Gomez-Cadenas *et al.*, Adv. High Energy Phys. **2014**, 907067 (2014).
- [62] F. Granena *et al.*, arXiv:0907.4054[hep-ex].
- [63] C. Licciardi, J. Phys. Conf. Ser. **888**, no.1, 012237 (2017).